Electronic Supplementary Material (ESI) for ChemComm.

Electronic Supplementary Information

Enhanced photoelectrochemical performance of internally porous Au-embedded α-Fe_2O_3 photoanodes for water oxidation

Pravin S. Shinde [a], Su Yong Lee,[b] Jungho Ryu,[c] Sun Hee Choi,*[,b] and Jum Suk Jang [a,*]

[a] *Division of Biotechnology, Safety, Environment and Life Science Institute, College of Environmental and Bioresource Sciences, Chonbuk National University, Iksan 570-752, Republic of Korea*

[b] *Pohang Accelerator Laboratory, Pohang University of Science and Technology (POSTECH), 80 Jigokro-127-beongil, Nam-gu, Pohang 37673, Republic of Korea*

[c] *Mineral Resources Research Division, Korea Institute of Geoscience and Mineral Resources, Daejeon 305-350, Republic of Korea.*

Corresponding Author(s):

*Email: shchoi@postech.ac.kr (SHC)

*E-mail: jangjs75@jbnu.ac.kr (JSJ)

Experimental details

Chemicals and materials. The used chemical reagents were Iron (II) sulfate heptahydrate ($FeSO_4 \cdot 7H_2O$, ≥98%, Alfa Aesar), Ascorbic acid, Amidosulfonic acid, Boric acid, Gold(III) chloride trihydrate ($HAuCl_4.3H_3O$, ≥99.9%, Aldrich), Cetyltrimethylammonium bromide (CTAB, $C_{19}H_{42}BrN$, ≥98.0%, Aldrich), Acetone, Absolute ethanol, and Ethanol, etc. Chemicals were used as-is without further purification. All the solutions were prepared using high purity deionized water (Scholar type, Human Power I+ Corp., Resistivity <18 MΩ cm). The iron films (to be converted to iron oxide) were prepared via PRED on conducting fluorine-doped tin oxide (FTO)-coated glass substrates (TEC7, 1 cm × 2.5 cm, 10−15 Ω cm^{-1}).

Materials synthesis. The iron films (to be converted to iron oxide) were prepared on clean FTO substrates via the pulse reverse electrodeposition (PRED) method. The cleaning of FTO substrates, the preparation of electrolyte, and the processing parameters used for PRED (square wave pulse amplitude of 10 V [−6/+4V], duty cycle of 20%, pulse period of 10 ms, and deposition time of 45 s) were kept according to our previous study.[1] A sulfate bath with or without CTAB served as the electrolyte for PRED. The CTAB concentration was 10 mM. The desired amount of surfactant was dissolved in a 50 mL sulfate bath, stirred for 10 min followed by ultrasonic treatment for 30 min, and obtained a clear and homogeneous solution. Solutions were made fresh for all the PRED experiments. Along with surfactant, the effect of in-situ incorporation of gold precursor (Au at%) was also studied. All PRED experiments were performed under identical conditions at room temperature, and at least three electrodes for each condition were prepared to assess the reproducibility of the films. As-grown films were blackish in color and reflected light. After deposition, the resulting films were rinsed with a abundant amount of deionized water and finally dried using a nitrogen stream. As-grown Fe films were then converted to iron oxide by a one-step HT-annealing method that involves quenching of the films in air after soaking them in a box furnace at 800°C for 13.5 min.[2] The iron oxide films appeared dark reddish brown, depending on the film thickness. The Fe_2O_3 film prepared using only surfactant (10 mM CTAB) was inhomogeneous, as shown in Figure S1, and hence was not characterized further. This also suggests that incorporation of gold during electrodeposition improves the strong attachment of as-grown film to the FTO substrate. The Fe_2O_3 films prepared by PRED using a 45 s deposition time without and with the incorporation of 7% gold alone and with 7% gold and 10 mM CTAB are denoted as F45, F45A7, and F45C10A7, respectively.

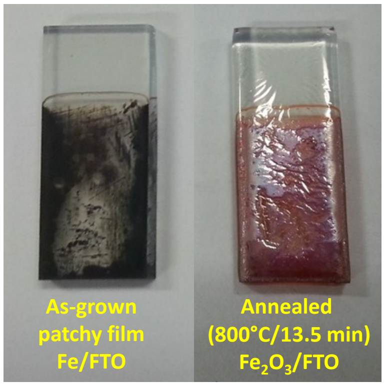

Scheme S1. Image of as-grown Fe and annealed Fe_2O_3 films synthesized on FTO by PRED under the F45C10 condition (i.e., with surfactant alone).

Characterization of materials. The representative Fe_2O_3 and Au-Fe_2O_3 samples were comprehensively characterized using several techniques. Structural properties of the photoanodes were examined using synchrotron X-ray diffraction (XRD) at 9C beamline of the Pohang Light Source II (PLS-II) in Korea. X-ray of 15.0 keV (λ=0.0827 nm) was selected by a Si(111) double crystal monochromator (DCM), and the standard theta-two theta (θ-2θ) XRD scan was carried out in the range of 20–70°. The element specific and amorphous phase-detectable X-ray absorption spectroscopy is applied to understand change in the local structure of Fe in Au-incorporated hematite. The X-ray absorption fine structure (XAFS) measurements were performed on the 7D beamline of the Pohang Accelerator Laboratory (PLS-II, 3.0 GeV). Synchrotron radiation was monochromatized using Si(111) double crystal monochromators. Spectra for the Fe K-edge (E_0=7112 eV) were taken under fluorescence mode at room temperature. X-ray absorption near edge (XANES) spectra and extended X-ray absorption structure (EXAFS) functions were obtained only for the representative samples. The incident beam was detuned by 15% at 7112 eV to attenuate the flux from higher order Bragg diffractions of silicon crystals in the monochromator. Its intensity was monitored using a He-filled IC SPEC ionization chamber and the fluorescence signal from the sample was measured with a PIPS (passivated implanted planar silicon) detector. ATHENA, from the IFEFFIT program suite, was used to analyze the obtained data for the local Fe structure in the Fe_2O_3 photoanodes.[3] The surface and cross-sectional morphologies of all the Fe_2O_3 films were examined on a Field Emission Scanning Electron Microscope (FESEM) (SUPRA 40VP, Carl Zeiss, Germany) equipped with an X-ray energy-dispersive spectrometer (EDS). The chemical state and elemental quantification of the freshly-synthesized iron oxide samples were performed using X-ray photoelectron spectroscopy (XPS) on a PHI Quantera II spectrometer equipped with a monochromatic Al Kα X-ray source ($h\nu$ = 1486.6 eV, 50 W, and 15 kV). The detection angle relative to the substrate surface was 45°. Wide survey spectra (binding energy, BE: 1200−0 eV) were recorded using an X-ray spot size of 200 μm at room temperature with an analyzer pass energy of 280 eV and an energy step size of 1 eV. High-resolution spectra in the region of interest were acquired with a pass energy of 55 eV and a step size of 0.1 eV. XPS data processing, including peak deconvolution, was performed using the XPS Peak-fit program with Shirley background subtraction and an iterative least-squares optimization algorithm. The high-resolution XPS spectra were calibrated by referencing the maximum of adventitious hydrocarbon peak at 284.8 eV. Deconvolution of the C1s and O1s peaks was performed according to their chemical environments. To observe Sn and Au incorporation into the representative Fe_2O_3/FTO photoanodes, full cross-sectional TEM samples were prepared with a dual-beam focused ion beam (FIB, Helios NanoLab, FEI) using a Ga+ ion beam source operating at 30 kV. Elemental analysis and elemental line profile mapping of the cross-sections were performed with a field-emission transmission electron microscope (JEM-2100F HR, JEOL) operating at 200 kV, equipped with an energy dispersive spectrometer (EDS). A UV-vis absorption study in the wavelength range from 350 to 800 nm was performed using a dual beam spectrophotometer (Shimadzu, UV-2600 series). The absorbance was measured using FTO as a reference.

Photoelectrochemical measurement. The water oxidation performance of the Fe_2O_3 photoanodes was measured in a PEC cell comprised of a three-arm glass compartment with a circular quartz window for light illumination. The PEC cell components included a Fe_2O_3/FTO photoanode as the working electrode, a Pt wire as the counter electrode, Ag/AgCl (saturated with KCl) as the reference electrode, and 1 M NaOH as the electrolyte. Standard simulated 1 sun (100 mW cm^{-2}, AM1.5G) illumination was provided using a solar simulator (Abet Technologies). All potentials mentioned in this work were originally measured with reference to the Ag/AgCl electrode (sat. KCl), and were translated to the reversible hydrogen electrode (RHE) scale using the Nernst equation (2):[4]

$$V_{\mathrm{RHE}} = V_{\mathrm{Ag/AgCl}} + 0.059\,p\mathrm{H} + V^{\mathrm{O}}_{\mathrm{Ag/AgCl}} \qquad \ldots (2)$$

where V_{RHE} was the converted potential vs. RHE, $V^{\mathrm{O}}_{\mathrm{Ag/AgCl}} = 0.1976$ V at 25 °C, and $V_{\mathrm{Ag/AgCl}}$ was the experimental potential against the Ag/AgCl electrode. The current–voltage (J–V), electrochemical impedance spectroscopy (EIS), and Mott–Schottky (MS) studies were performed using a potentiostat (Ivium, Netherland) equipped with an electrochemical interface and impedance analyzer facility. EIS was performed to investigate the charge-transport properties under 1 sun illumination at 1.23 vs. RHE (V_{RHE}). The experimental EIS (real *vs.* imaginary impedance) data was validated using the Kramers–Kronig transform test and fitted to a suitable equivalent circuit model using the ZView (Scribner Associates Inc.) program. MS (C_{sc}^{-2} *vs.* V) measurements were performed in the dark with an applied DC potential window of –0.6 to 0.7 V vs. Ag/AgCl at 0.5 kHz AC frequency. The amplitude of the AC potential was 10 mV in both EIS and MS measurements. The carrier concentration or donor density (N_D) was estimated from the slope in the quasi-linear region of the MS plot (C_s^{-2} *vs.* V) near the flat band potential (V_{fb}) according to the relation (a):[5]

$$N_D = (2/e_o\varepsilon\varepsilon_o)\,[d(C_s^{-2})/dV] \qquad \ldots (1)$$

where e_o the electron charge, ε the dielectric constant of hematite (80), ε_o the permittivity of vacuum, C_s is the space charge layer capacitance, and V is the potential applied at the electrode. Smaller slope is accounted for larger N_D value.

Crystallite size of the hematite film was evaluated using the Scherer equation as follows.

$$D_{hkl} = \frac{K_S\lambda}{\beta_{hkl}cos\theta} \qquad \ldots (2)$$

where D_{hkl} is the crystallite size along the direction perpendicular to a (*hkl*) plane, K_S is the Scherrer constant of 0.829, β_{hkl} is the full width at half maximum (FWHM) of the peak from a (*hkl*) plane, θ is the Bragg angle. Bragg peak of H(104) was used for the Scherrer analysis since it was the most intense one among the hematite peaks, and position and FWHM were measured by fitting the peak with the Pearson-VII function.

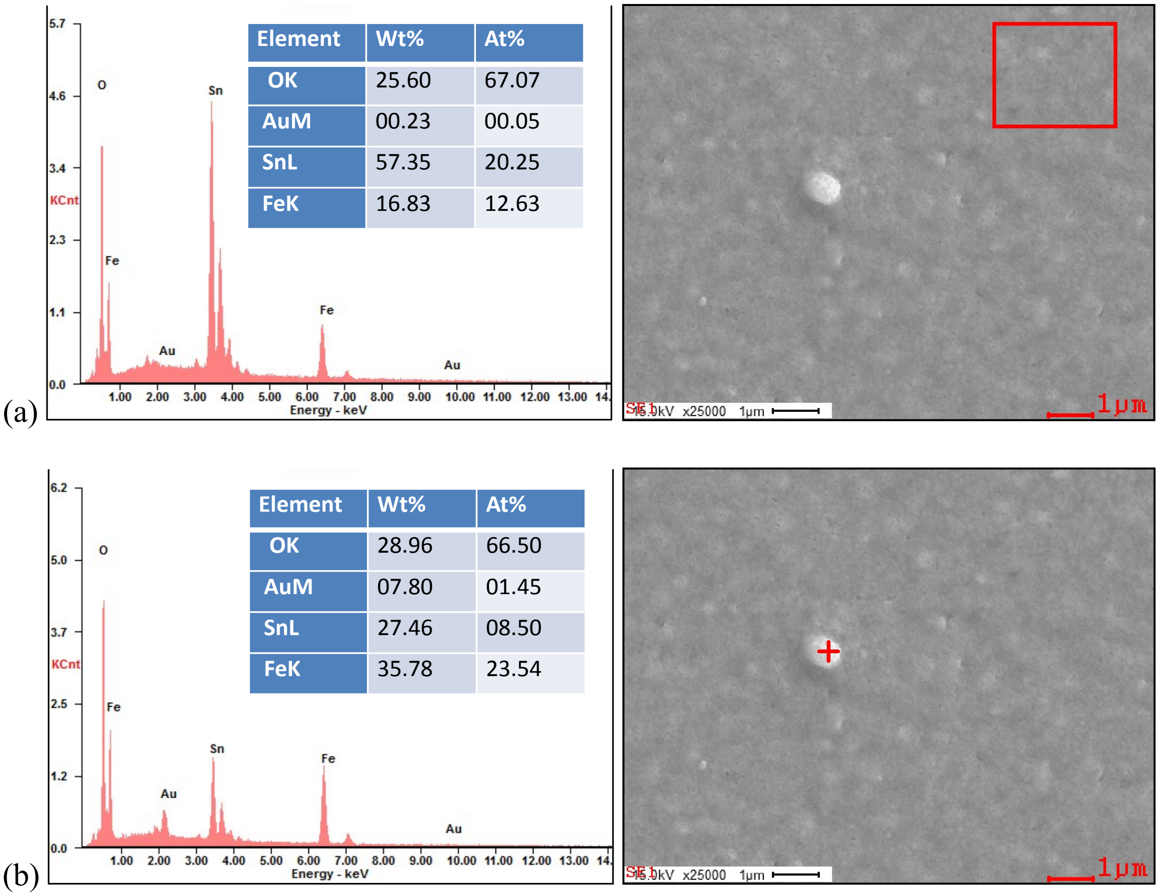

(a)

Element	Wt%	At%
OK	25.60	67.07
AuM	00.23	00.05
SnL	57.35	20.25
FeK	16.83	12.63

(b)

Element	Wt%	At%
OK	28.96	66.50
AuM	07.80	01.45
SnL	27.46	08.50
FeK	35.78	23.54

Figure. S2. EDX spectrum of a F45C10A7 hematite sample prepared at 800°C for 13.5 min: (a) Area EDS and (b) Point EDS at an Au aggregate.

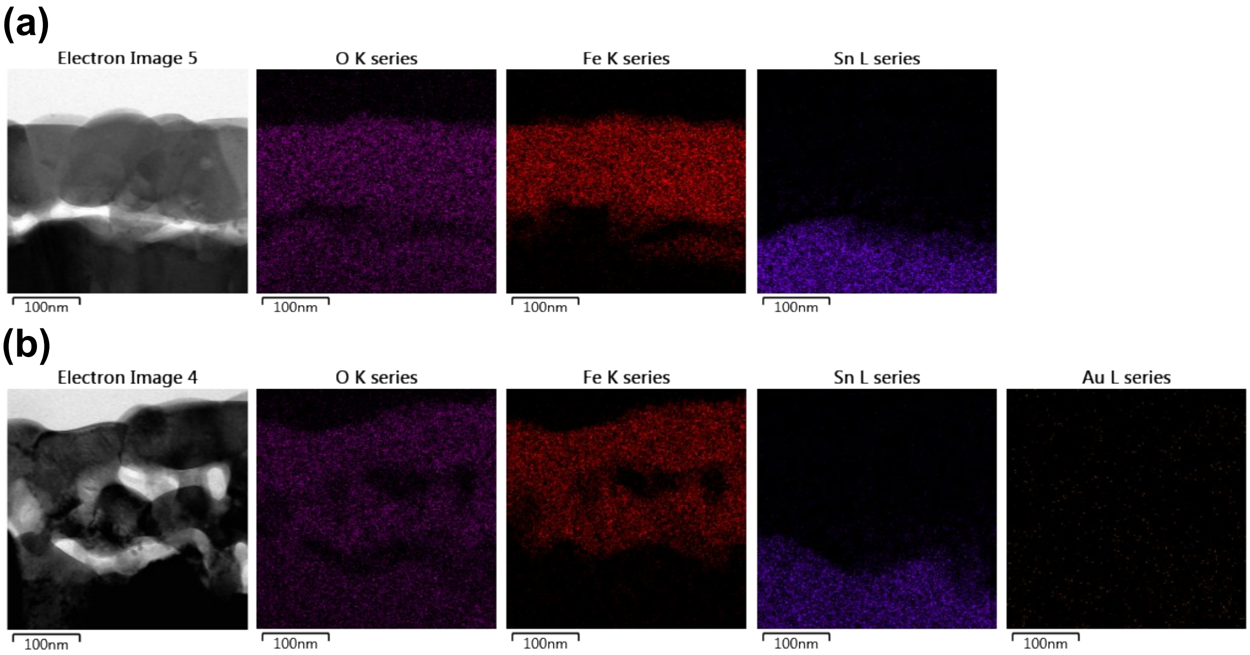

Figure. S3. EDS mapping of cross-sectional FIB TEM specimen of (a) F45 and F45C10A7 samples.

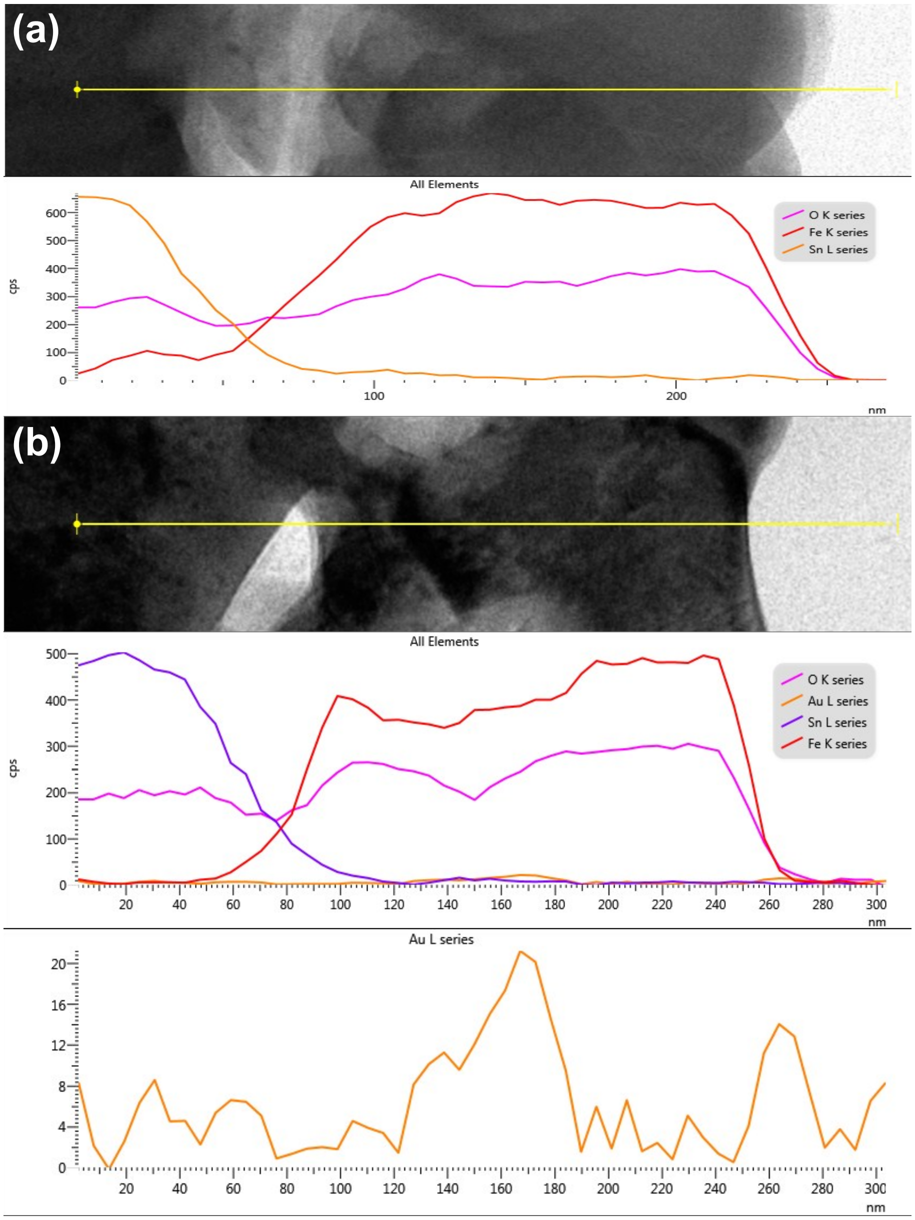

Figure. S4. EDS line mapping of cross-sectional FIB TEM specimens of (a) F45 and (b) F45C10A7 samples

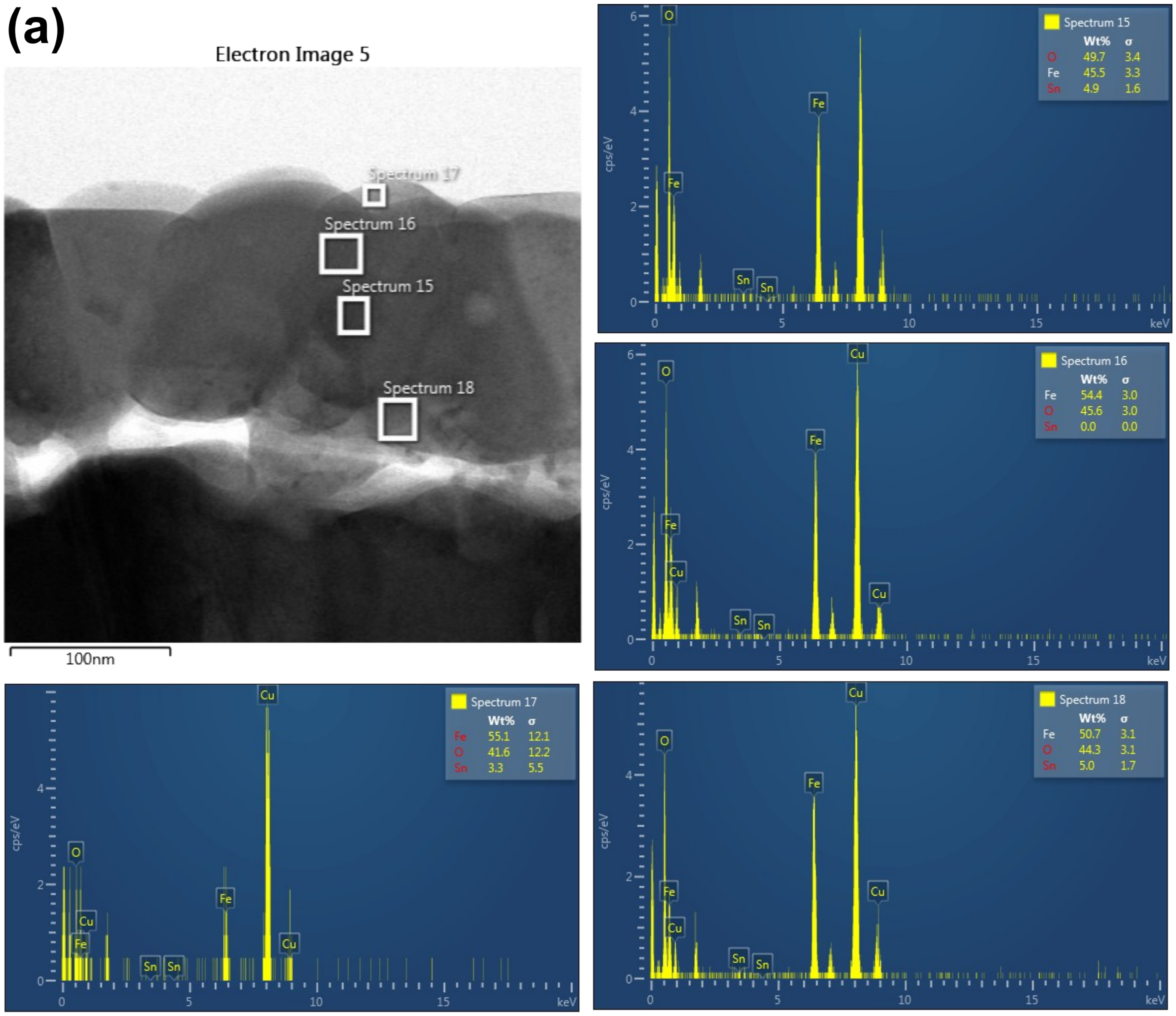

Figure. S5(a) Cross-sectional TEM micrograph of an annealed F45 sample with point EDS spectra revealing the % compositions of the elements Fe, O, and Sn.

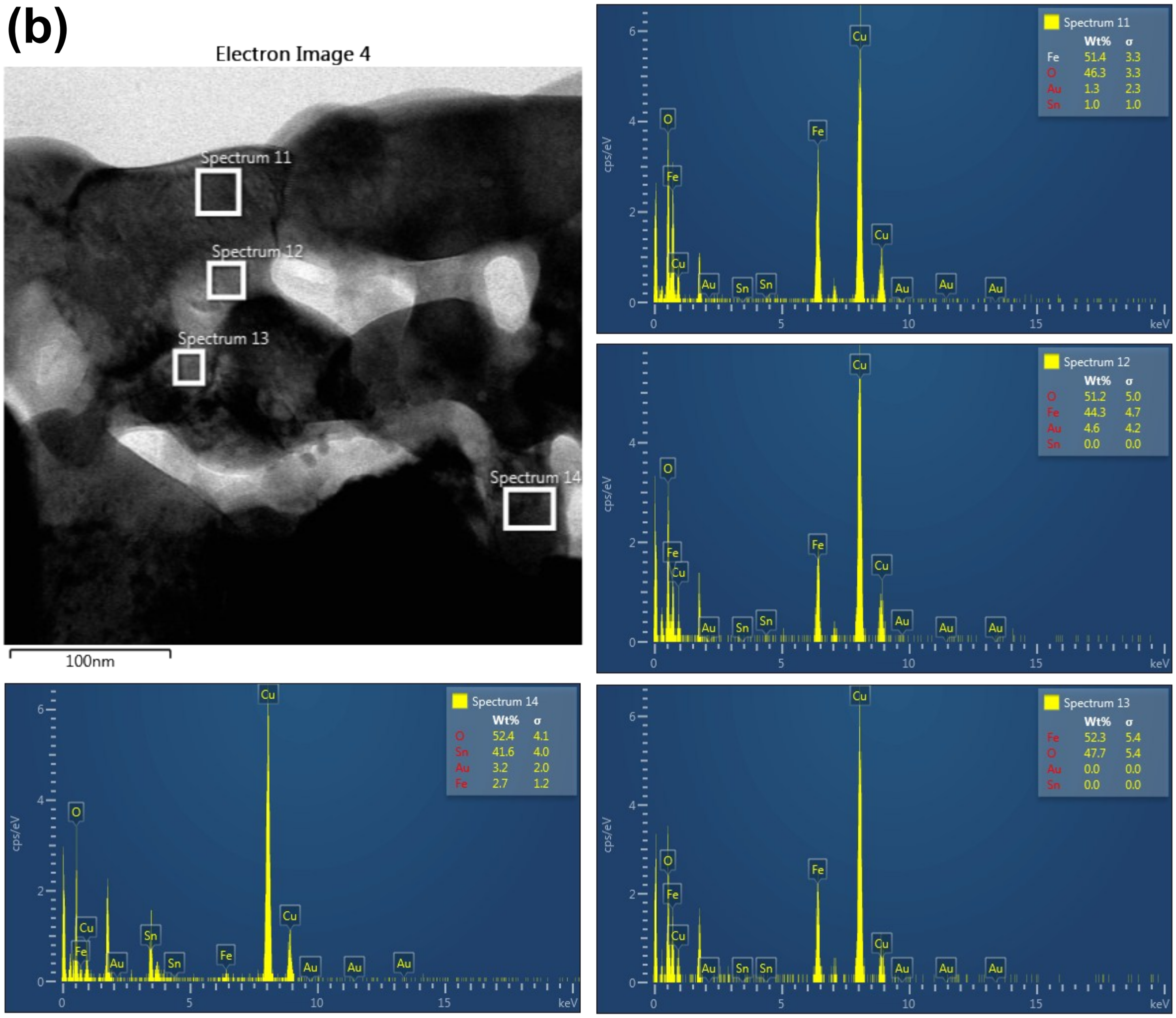

Figure. S5(b) Cross-sectional TEM micrograph of an annealed F45C10A7 sample with point EDS spectra revealing the % compositions of the elements Fe, O, Sn, and Au.

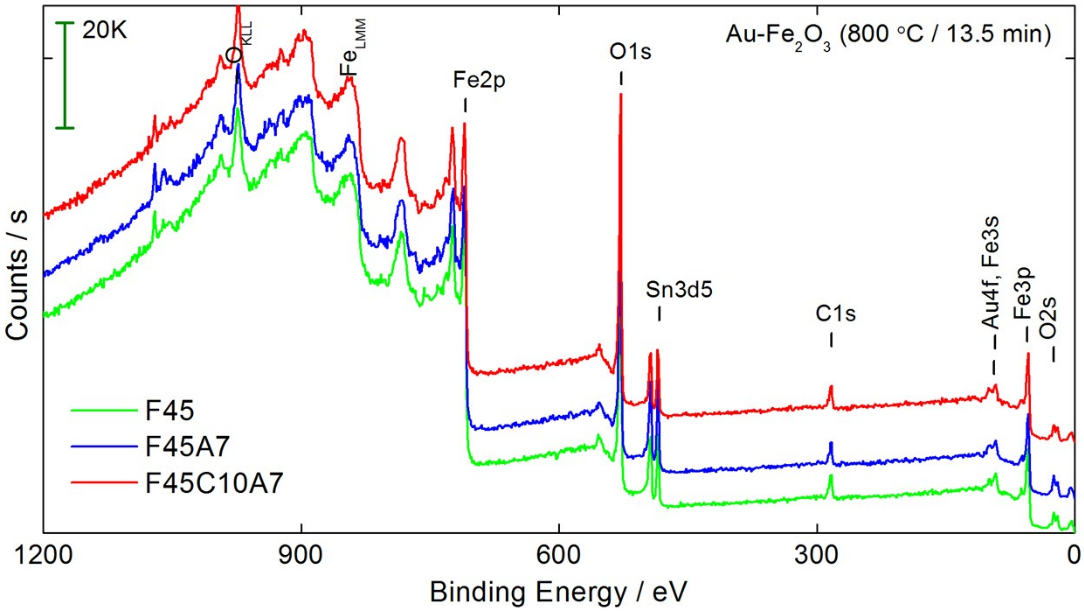

Figure. S6. Survey XPS spectra of F45, F45A7, and F45C10A7 hematite samples.

Table S1. Elemental ID and quantification of Fe_2O_3 films synthesized with or without Au and surfactant, and annealed at 800 °C for 13.5 min. The peak values were calibrated with reference to adventitious carbon at 284.8 eV.

Samples/	Fe 2p		O 1s		Sn 3d5		Au 4f	
Parameters	BE	at.%	BE	at.%	BE	at.%	BE	at.%
F45	710.8	67.97	529.7	30.26	486.1	1.77	84.0	0.00
F45A7	710.8	65.74	529.7	31.95	486.1	2.30	84.0	0.00
F45C10A7	710.8	65.54	529.7	32.78	486.1	1.68	84.0	0.00

Note: About 14-17 at% carbon (C1s) is detected in annealed samples due to atmospheric impurities and it is not considered in the above table.

Table S2. Structural parameters calculated form Fe K-edge EXAFS fits for Fe_2O_3 films synthesized with or without Au and surfactant.

	R_1 (Å)[a]	R_2 (Å)[b]	σ^2 ($Å^2$)[c]	R-factor[d]
F45	1.939	2.109	0.0032(7)	0.010
F45A7	1.962	2.134	0.0032(8)	0.010
F45C10A7	1.955	2.126	0.0034(6)	0.009

[a,b] Fe-O bond distance (uncertainty < 0.005), [c] Debye-Waller factor (indicator of the structural disorder), [d] a sum-of-squares measure of the fractional misfit.

The numbers in parentheses in the column marked with a *c* denote uncertainty of the calculated parameter at the last digit place.

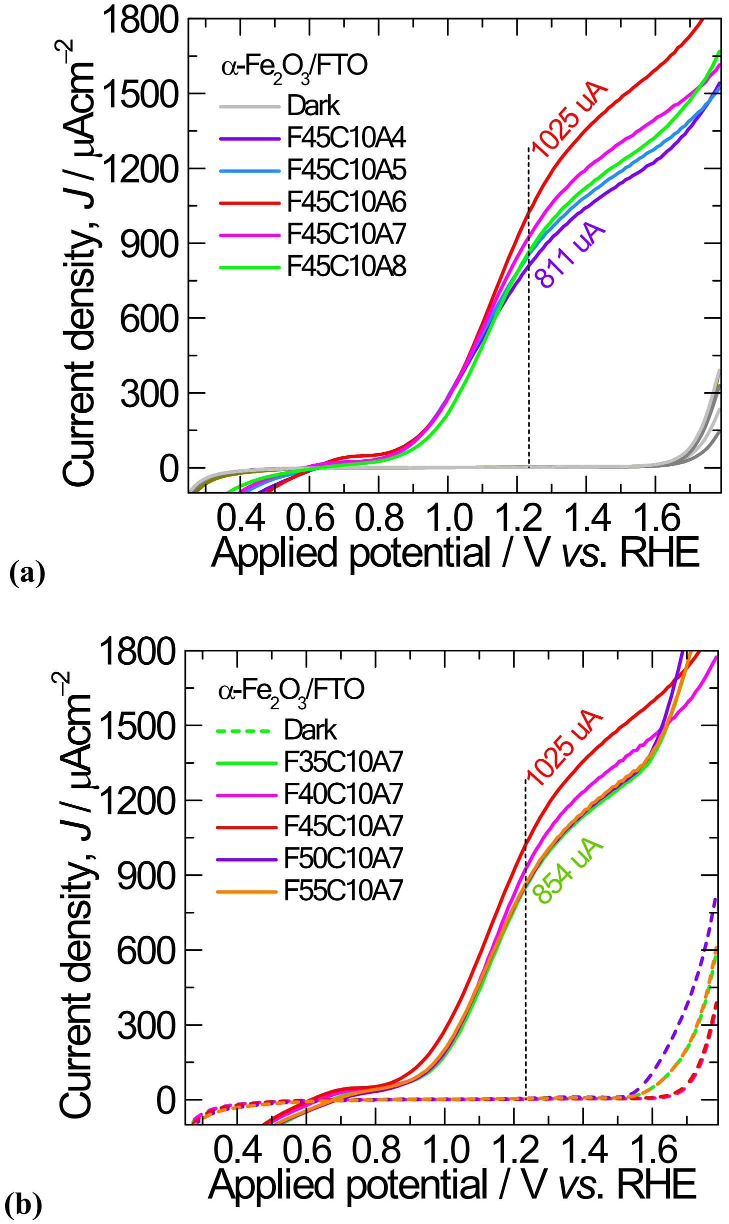

Figure. S7. Current-voltage (*J-V*) characteristics of hematite photoanodes made (a) with a 45 s PRED time with different Au concentrations of 4, 5, 6, 7 and 8%; and (b) with a fixed Au concentration of 7% and different PRED times (film thicknesses). All photoanodes were fabricated at 800°C for 13.5 min. The *J-V* curves were recorded at a scan rate of 50 mV s^{-1} under 1 sun illumination in 1 M NaOH electrolyte.

Table S3 The electrochemical parameters obtained from Nyuist and Mott-Schottky plots for hematite samples.

Samples/ Parameters	R_s (Ω)	R_{trap} (Ω)	C_{CPE1} (F)	R_{ct} (Ω)	C_{CPE2} (F)	V_{fb} (V_{RHE})	N_D (cm^{-3})
F45	43.79	51.91	46.263×10^{-6}	434.1	3.7864×10^{-6}	0.481	0.7467×10^{20}
F45A7	62.80	81.88	49.875×10^{-6}	637.8	4.6508×10^{-6}	0.455	0.4878×10^{20}
F45C10A7	38.38	10.93	60.925×10^{-6}	204.6	9.3725×10^{-6}	0.513	3.2940×10^{20}

Supplementary References

1 P. S. Shinde, A. Annamalai, J. Y. Kim, S. H. Choi, J. S. Lee and J. S. Jang, J. Phys. Chem. C, 2015, 119, 5281.

2 P. S. Shinde, A. Annamalai, J. H. Kim, S. H. Choi, J. S. Lee and J. S. Jang, Sol. Energ. Mater. Sol. Cells, 2015, 141, 71.

3 B. Ravel and M. Newville, J. Synchrotron Radiat., 2005, 12, 537.

4 A. Kay, I. Cesar and M. Grätzel, J. Am. Chem. Soc., 2006, 128, 15714.

5 A. A. Tahir, K. U. Wijayantha, S. Saremi-Yarahmadi, M. Mazhar and V. McKee, Chem. Mater., 2009, 21, 3763.